Recording Neuronal Activity On Chip with Segmented 3D Microelectrode Arrays

Revyn, Nele; Hu, Michel H.Y.; Frimat, Jean-Philippe; de Wagenaar, Bjorn; van den Maagdenberg, Arn M.J.M.; Sarro, Pasqualina M.; Mastrangeli, Massimo

DOI
10.1109/MEMS51670.2022.9699597

Publication date
2022

Document Version
Final published version

Published in
Proceedings of the 2022 IEEE 35th International Conference on Micro Electro Mechanical Systems Conference (MEMS)

RECORDING NEURONAL ACTIVITY ON CHIP WITH SEGMENTED 3D MICROELECTRODE ARRAYS

Nele Revyn[1], Michel H. Y. Hu[2], Jean-Philippe M. S. Frimat[2], Bjorn De Wagenaar[1], Arn M. J. M. van den Maagdenberg[2], Pasqualina M. Sarro[1] and Massimo Mastrangeli[1]
[1]ECTM, Department of Microelectronics, TU Delft, THE NETHERLANDS
[2]Human Genetics and Neurology, Leiden University Medical Centre, THE NETHERLANDS

2022 IEEE 35th International Conference on Micro Electro Mechanical Systems Conference (MEMS) | 978-1-6654-0911-7/22/$31.00 ©2022 IEEE | DOI: 10.1109/MEMS51670.2022.9699597

ABSTRACT

We present preliminary recordings on chip of three-dimensional (3D) electric neuronal activity from cultures of cortical neurons derived from human-induced pluripotent stem cells (hiPSCs). The recordings were obtained through 3D microelectrode arrays (MEAs) composed of truncated, 90 µm-high Si micropyramids endowed with multiple, electrically distinct, and vertically arranged TiN microelectrodes. The unique design and implementation of the 3D microelectrodes, complemented by a 60-electrode readout interface, allow for 3D spatial recording of neuronal activity, as well as single-unit recordings in high throughput, which are currently not possible with commercial MEA platforms. Future work will aim at optimizing extended 3D MEAs over optically transparent substrates for electro-physiological investigation of 3D neuronal tissues and organoids.

KEYWORDS

brain-on-chip, electrodes, electrophysiology, microelectrode array, microfabrication, neurons, organ-on-chip.

INTRODUCTION

Microelectrode arrays (MEAs), composed of dense sets of spatially arranged microelectrodes, are powerful and established tools to study *in vitro* the electrophysiology of electrogenic cell cultures, in particular to continuously measure and spatially track their collective and distributed activity [1]. Standard and most common MEAs are planar and lack topography, and can mainly sample extracellular electrophysiological signals from the surface of cells and tissues. Limiting the electrode impedance and enhancing the biomechanical and electrical coupling between electrodes and cells are critical features to achieve accurate and reliable readouts for MEAs. Many studies have been carried out on electrodes materials and geometries suitable to improve the electrode-cell interfacing [1-3], including *e.g.* mushroom-shaped electrodes [4], electroplated gold pillars [5], and boron-doped diamond pillars [6]. MEAs represent a prime vehicle for studying specifically the behavior and pharmacological response of neuronal cell cultures as relating to *e.g.* highly debilitating pathologies such as migraine and cortical spreading depolarization [7-8]. However, quantifying the full extent of neuronal interactions in a three-dimensional (3D) tissue requires recording along all three spatial dimensions [1, 3]. Promising results for 3D *in vitro* recording were reported [1, 3], *e.g.* by fabricating a segmented planar (2D) microelectrode array to be deployed in the third spatial dimension by mechanical actuation [9]. In this work we show direct, wafer-level microfabrication of arrays of microelectrodes allocated across all three spatial dimensions. This is achieved by patterning Si micropyramids [10] with individually addressable and vertically stacked TiN microelectrodes on their sloped facets, and interfacing the arrays with standard readout systems.

DESIGN AND FABRICATION PROCESS

The proposed 3D MEAs were designed as 5-by-4 arrays of truncated, ~90 µm-high square Si micropyramids with 20 µm-wide flat top plateau and slope of lateral facets ranging from 46º to 53º (Fig. 1a). Each micropyramid features three independent, externally addressable microelectrodes (Fig. 1b), totaling 60 microelectrodes per array.

The microfabrication of the 3D MEAs consists of two main parts: micromachining of truncated Si micropyramids (*i.e.*, frusti), and patterning of multiple microelectrodes over the micropyramids' facets. The truncation of the apex of the micropyramids was introduced to prevent the otherwise sharp and rigid tips from potentially damaging the neuronal tissue, as well as to host a single flat microelectrode sampling point. In this regard, the frustum geometry is appealing to single neuron studies, as it introduces the possibility of pinpointing a single neuron on the single topmost electrode and thus measure the activity of a roughly isolated cell. The rest of the microelectrodes in the MEAs were designed to capture multi-cell electric network activity at different tissue depths.

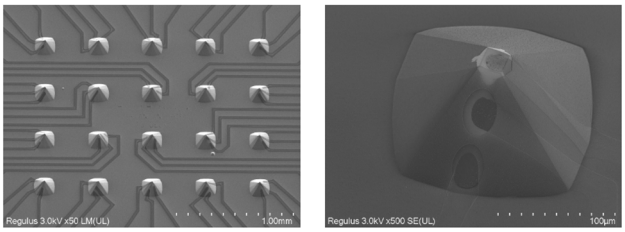

Figure 1: A) SEM micrograph of a 3D MEA, featuring 20 Si micropyramids and 60 TiN electrodes in total. B) Each micro-pyramid features 3 distinct, vertically stacked microelectrodes.

The full fabrication process of the 3D MEAs is shown in Fig. 2. First, a ~400 nm-thick silicon nitride layer was deposited on a 4" silicon wafer by low-pressure chemical vapor deposition, and then patterned using photolithography of positive tone photoresist and C_2F_6-based dry etching (Fig. 2a). The patterned SiN layer was used as a hard mask during subsequent anisotropic wet etching of the Si substrate (Fig. 2b). The etching was conducted in a water solution of 25% v/v tetramethylammonium hydroxide (TMAH) at 80°C using Triton as additive surfactant. TMAH etches silicon anisotropically, with the fastest etching planes being (100) [11]. The addition of the surfactant influences the selective etch rates of silicon crystal planes

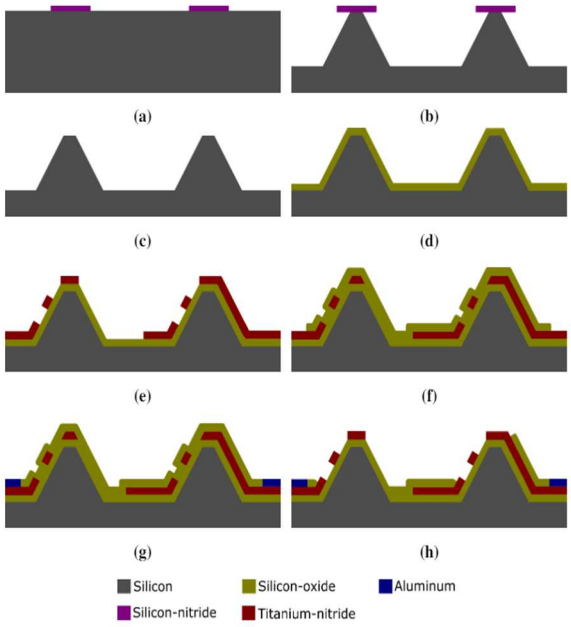

Figure 2: Fabrication process: A) Patterning of a one-side polished 4" Si wafer with a SiN hard mask. B) Timed anisotropic wet etching of Si (25% TMAH + Triton). C) Removal of the hard mask. D) Passivation of the wafer surface with thermally grown SiO_2. E) Patterning of TiN to define electrodes and interconnects. F) Surface passivation with SiO2, with openings for TiN electrode tips. G) Patterning of Al to define pads for wire-bonding. H) Opening of the second passivation layer to finalize the sampling points. Thickness of layers not to scale.

in such a way that arrays of pyramidal structures can be obtained more conveniently. In particular, the (110) planes are etched more slowly than without the additive, whereas the etch rate of (100) planes remains unaltered [11]. Thence, surfactant addition drastically reduced hard mask undercut during etching, enabling better etch control and the option of closer spacing (*i.e.*, smaller pitch) of micropyramids. The smoothness of the etched silicon surface is also improved by Triton addition to the etch solution [11]. The SiN hard masking layer was patterned into square-shaped patches oriented by design along the (110), (120) and (130) crystal Si planes, respectively. Fig. 3 shows how crystal plane selection by hard mask design and orientation with respect to the wafer flat of a (100) Si wafer led to anisotropic etch of micropyramids with different slope angles for the lateral facets. Common etch-stop techniques – such as landing on *e.g.* a buried oxide or boron-doped layer, or an electrochemical etch stop [12] – were considered unsuitable to determine the desired pyramidal shape. Therefore, the wet etching was timed to result in around 90 µm-high micropyramids, with width of the top plateau of around 20 µm and lateral facet slope ranging from 46° to 53° according to hard mask orientation. Each array consisted of 20 micropyramids with center-to-center pitch of 460 µm along both main directions. After completion of the Si etch, the SiN hard mask was removed by wet etching in a phosphoric acid solution at 157 °C (Fig. 2c).

After electrically passivating the full surface of the substrate with a 400 nm-thick layer of thermally-grown

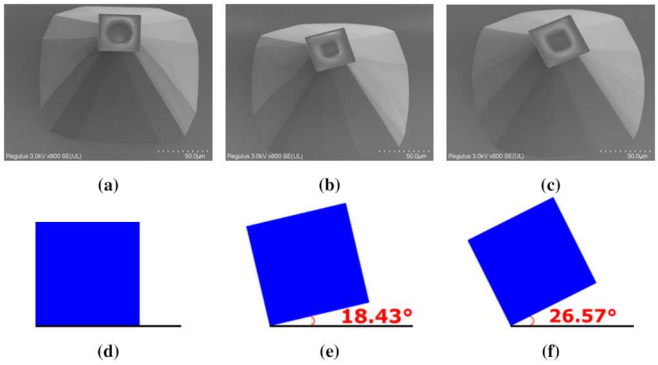

Figure 3: (a-c) SEM micrographs of 90 µm-high Si micropyramids wet-etched using hard masks oriented respectively along the (110), (120) and (130) Si crystal planes (note the SiN layer still attached to the micropyramid). (d-f) Respective mask orientations compared to the wafer flat.

SiO_2 (Fig. 2d), a 10nm/150nm-thick Ti/TiN layer was sputtered at 1kW and lithographically patterned to define the microelectrodes. The relatively high substrate topography present by this stage and the need to pattern microelectrodes on the slopes of the micropyramids motivated the use of photoresist spray-coating for the subsequent photolithographic patterning step. Spray coating tended to produce uneven resist deposition, even after the multiple deposition steps required for continuous surface coverage. Particularly, the applied resist layer appeared thinner at the concave corners present around the flat top micropyramid facets, and it tended to puddle into thicker deposits at the convex corners located at base of the micropyramids. To a non-uniform resist thickness should in principle correspond a locally adapted exposure time and mismatched development to obtain consistent photolithography results. In addition, the design and test of multiple micropyramid orientations and accordingly different microelectrode patterns made the 3D MEA chips on the wafer not identical. Hence an optical mask aligner had to be used in place of a stepper to expose the substrate. In soft contact lithography executed with a contact mask aligner, Fresnel diffraction of UV light in gaps between the mask and the wafer surface can deteriorate resolution of patterns in the cavities [13]. Careful photoresist patterning addressed all mentioned aspects and trade-offs. The TiN layer was dry-etched using Cl_2- and HBr-based plasma (Trikon Omega 201) (Fig. 2e).

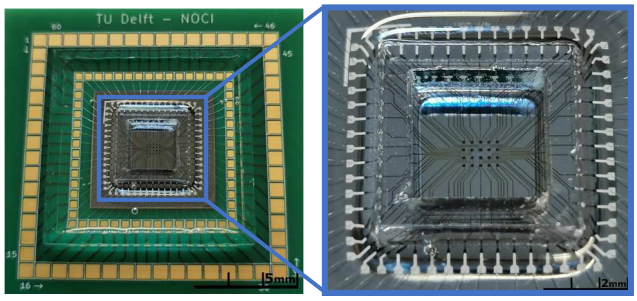

Figure 4: A) Full assembly of the 3D MEA chip onto a custom PCB with 60-electrodes MEA layout. B) Close-up view of chip packaging, including wire bonding and assembly of a transparent polyacrilate square well by means of transparent biocompatible glue.

The substrate was then electrically passivated with a 400 nm-thick layer of SiO_2 deposited by plasma-enhanced chemical vapor deposition (PECVD) (Fig. 2f). Windows in this passivation layer were first opened by masked dry etching at the far ends of the TiN interconnects on the periphery of each array. Contact pads for wire bonding were formed within these windows through subsequent evaporation and patterning of a 1 µm-thick layer of Al (Fig. 2g).

Finally, the PECVD oxide layer was additionally opened using lithographic patterning and wet etching in a buffered hydrofluoric acid solution to locally expose the tips of the TiN microelectrodes (Fig. 2h). This finalized the microfabrication of vertically stacked and electrically independent sampling points on each pyramid (Fig. 1b).

After full fabrication, 18 by 18 mm² chips were diced out of the processed wafers and wire-bonded to square printed circuit boards (PCBs), whose 60 peripheral contact pads were designed for compatibility with the commercially available MEA2100 readout system from Multichannel Systems (Fig. 4a) [14]. As mentioned, each die included a 5-by-4 array of micropyramids, each micropyramid featuring 3 independent microelectrodes (Fig. 1b). After wire-bonding, the center of the Si chip was demarcated by a transparent polyacrylate square well, glued to the chip using Loctite Hysol M-32L Medical Epoxy glue (Fig. 4b). The same glue was used to fully seal the wire bonds and protect them during chip use in incubator environments.

EXPERIMENTAL RESULTS

The fabricated and packaged 3D MEAs were tested for electrical functionality prior to *in vitro* biocompatibility and preliminary cell culture tests. The electrical characterization was executed using two setups: the MEA2100 readout system, and an electrochemical setup with reference, counter and working electrodes in phosphate buffered saline (PBS). The *in vitro* experiments were carried out using cortical neurons derived from human-induced pluripotent stem cells (hiPSCs).

Electro-chemical characterization

The microelectrodes' background noise was quantified by means of the MEA2100 readout system, which was used to measure the voltage readout from the microelectrodes while being submerged in cell culture media. The background noise resulted in the range of 10 to 20 µV.

Electrochemical impedance spectroscopy (EIS) was carried out to estimate the microelectrode impedance. During EIS measurements, magnitude and phase of an electrode's impedance are tracked on the counter electrode as a response to the excitation of the working electrode by means of a voltage (or current) driving signal over a range of frequencies [15, 16]. As illustrated in Fig. 5, in our setup a single 3D MEA chip was submerged in 0.1M PBS together with a miniature leakless Ag/AgCl reference electrode and a Pt auxiliary electrode. During the measurements, the TiN microelectrodes under test represented the working electrodes of the electrochemical cell, and were connected to the measurement system through a wire soldered to the PCB. We used a sinusoidal waveform with amplitude V_{RMS} of 20 mV and frequency ranging from 10 Hz to 10 kHz as driving input. Three representative measured

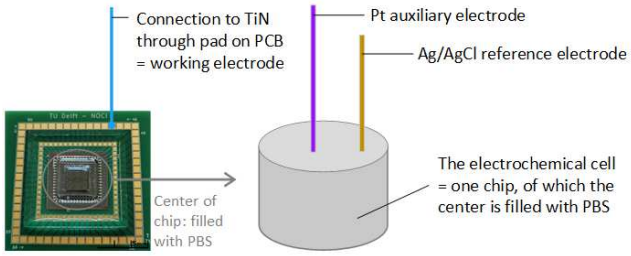

Figure 5: Setup of EIS measurements. The center of the chip, containing the TiN electrodes on the micropyramids, and demarcated by the transparent well, was filled with 0.1M PBS. A Pt auxiliary and Ag/AgCl reference electrode were also submerged in the PBS contained in the well. The TiN microelectrode under test was used as working electrode of the electrochemical cell, and was connected to the measurement unit through the readout pads on the PCB.

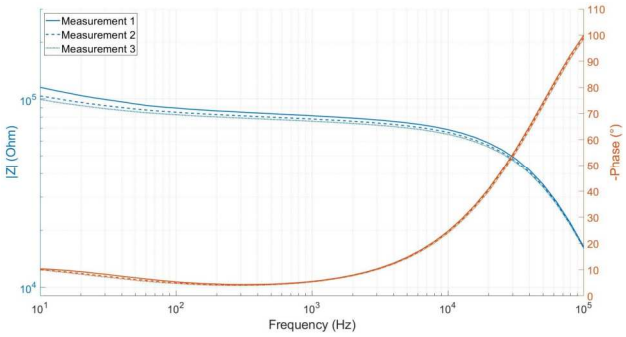

Figure 6: EIS of a single Ti/TiN electrode on the 3D MEA in 0.1M PBS with a Pt auxiliary and Ag/AgCl reference electrode, showing impedance of ~$10^5\Omega$ at 1kHz and capacitive effects at higher frequencies.

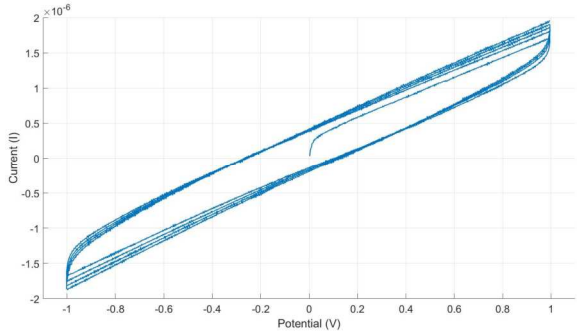

Figure 7: Result of cyclic voltammetry measurement of a single Ti/TiN electrode on the 3D MEA in 0.1M PBS with Pt auxiliary and Ag/AgCl reference electrode., showing the ability to store charge.

spectra are displayed in Fig. 6. The microelectrodes exhibited an impedance in the range of 30 kΩ to 500 kΩ under 1 kHz excitation frequency.

Using the same 3-electrode setup as for the EIS measurements, electrode characterization by cyclic voltammetry was also executed. The preliminary result displayed in Fig. 7 shows that the microelectrodes can also store charge, an important characteristic for eventual use of the electrodes for stimulation alongside recording of neural activity.

Experiments with cells

Cortical neurons derived from hiPSCs were differentiated and matured on the 3D MEAs following Stemcell Technologies' protocol. We monitored the 3D neuronal cultures grown on these structures up until 25 days *in vitro* (DIV), and used custom scripts to assess their electrophysiology. Fluorescence imaging showed that neurons progressively grow, crawl over and move across the facets of micropyramids (Fig. 8), and that single neurons can be secluded on the micropyramid plateaus, prompting the possibility of single-unit recording. This could open the possibility to use the electrodes on the side facets for multi-unit recordings to assess the whole network, while the electrodes on the micropyramid plateaus can be used to assess local areas within the network. Measurements by means of the 3D MEAs did show clear network bursting activity, evidence of neurons viability on chip (Fig. 9).

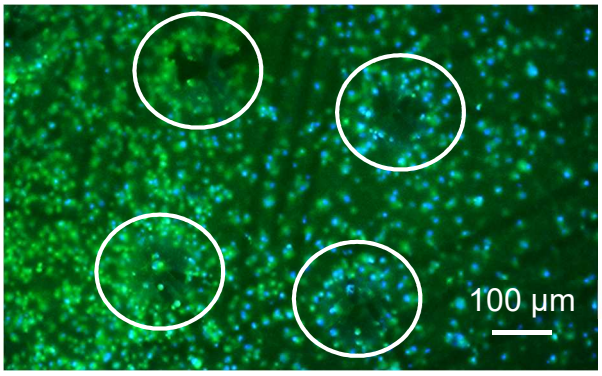

Figure 8: Full-focus image of hiPSC-derived cortical neurons on a 3D MEA. White circles highlight neurons growing on the micropyramids.

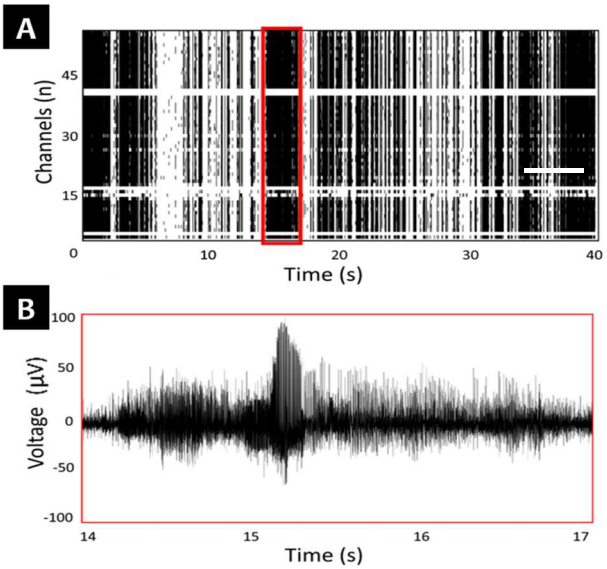

Figure 9: Measuring neuronal activity on 3D MEA chip. A) Spike raster plot (network burst highlighted in red) and B) single-channel trace of a 3D MEA recording with hiPSC-derived cortical neurons matured for 25 days on the 3D MEA chip.

CONCLUSION

We recorded and analyzed 3D neuronal activity on chip using wafer-level fabricated arrays of truncated Si micropyramids patterned with electrically distinct and vertically-stacked TiN electrodes. Encouraging preliminary results from recording activity of cortical neurons by means of the 3D MEAs prompt further analyses and future experiments, envisaged with brain organoids or 3D cell constructs, to record full 3D electrical neuronal network activity in 3D. Future work will also investigate the adoption of softer and transparent substrates for the 3D structures to enhance respectively physiological realism and continuous optical monitoring of cell cultures on the chips.

ACKNOWLEDGEMENTS

The authors would like to thank the staff at the Else Kooi Laboratory of TU Delft for their support, and Tim de Rijk for his early contributions to the project.

This work was supported by the Netherlands Organ-on-Chip Initiative, an NWO Gravitation project funded by the Ministry of Education, Culture and Science of the government of the Netherlands (024.003.001), and by the "Moore4Medical" project funded by the ECSEL Joint Undertaking under grant agreement H2020-ECSEL-2019-IA-876190.

REFERENCES

[1] C. M. Didier *et al.*, *J. Micromech. Mircroeng.*, 30, pp 103001, 2020.
[2] G. H. Kim *et al.*, *Materials*, 11(10), pp 1995, 2018.
[3] J. S. Choi *et al.*, *Biosens, Bioelectron*, 171, pp 112687, 2021.
[4] S. Ojovan *et al.*, *Sci Rep*, 5, pp 14100, 2015.
[5] M. Cabello *et al.*, *Proc. 2018 Spanish Conference on. Electron Devices (CDE 2018)*, Salamanca (ES).
[6] G. Piret *et al.*, *Biomaterials*, 53, pp 173-183, 2015.
[7] J. J. Theriot *et al., J. Neurosci*. 32(44), pp. 15252–15261, 2012.
[8] M. D. Ferrari *et al.*, *Lancet Neurol.* 4(1), pp. 65-80, 2015.
[9] D. A. Soscia *et al.*, *Lab Chip*, 20(5), pp. 901-911, 2020
[10] M. M. Smiljanic *et al.*, *Micromachines*, 10(2), pp 102, 2019.
[11] M. A. Gosvalez *et al.*, *J. Micromech. Mircroeng*., 19, pp 125011, 2009.
[12] S. D. Collins, *J. Electrochemical Society*, 144(6), pp 2242, 1997.
[13] Z. K. Esfahani, *PhD thesis*, TU Delft, January 2017.
[14] Multichannel Systems MCS GmbH, available at: https://www.multichannelsystems.com/products/mea2100-systems (accessed: 08/11/2021).
[15] C. Boehler *et al.*, *Nature Protocols*, 15, pp 3557-3578, 2020.
[16] S. F. Cogan, *Annual Review of Biomedical Engineering*, 10, pp 275-309, 2008.

CONTACT

*M. Mastrangeli, m.mastrangeli@tudelft.nl